

## $^{57}\text{Fe}$ -Mössbauer analysis of biological and synthetic Fe/S clusters

Jaeun Hwang and Jaehong Han\*

Metalloenzyme Research Group and College of Biotechnology and Natural Resources,  
Chung-Ang University, Anseong 456-756, Republic of Korea

(Received 21 January 2015; accepted 9 March 2015)

**Abstract** - Biological Fe/S clusters play various important roles, such as electron transfer and substrate transformation. In the study of the electronic properties of biological and chemical Fe/S clusters,  $^{57}\text{Fe}$ -Mössbauer spectroscopy provides imperative information. In this review, practical aspects of  $^{57}\text{Fe}$ -Mössbauer spectroscopy, with an emphasis on the isomer shift  $\delta$ , were discussed. The isomer shift values of the various biological Fe/S proteins and the synthetic Fe/S complexes at different oxidation states and electronic spin states, along with the related Mo/Fe/S and Fe carbonyl clusters, were reviewed. From the Mössbauer isomer shift, the physical properties of the Fe center in the Fe-enzymes can be obtained. In addition, the binding of the substrate or inhibitor to the active Fe center can be monitored.

**Keywords:** Bioinorganic, electronic spin, Fe/S cluster, Mössbauer, oxidation state, spectroscopy.

### 1. Introduction

Bioinorganic research often relies heavily on extensive spectroscopic analysis. Sometimes, the accessibility, measurement, and interpretation of such analyses are not so easy for those whose major is not chemistry. Perhaps, Mössbauer spectroscopy is one of them. Only a few Mössbauer spectrometers are available for researchers worldwide, and interpretation of spectra can only be carried out by an expert. However, Mössbauer spectroscopy provides a very important piece of information about Fe-containing enzymes, which cannot be otherwise obtained from other spectroscopy, like NMR or EPR. Therefore, it is very important to be able to evaluate and interpret the experimental and published data when the research is related to Fe-containing proteins or compounds. There are some monographs and review papers covering the general aspects of Mössbauer spectroscopy (Filatov, 2009; Güttlich *et al.*, 1978; Vertes *et al.*, 1979). In this review, practical aspects of  $^{57}\text{Fe}$ -Mössbauer analysis of the Fe/S and Mo/Fe/S clusters found in biology and synthesized in inorganic chemistry were mainly discussed. Its aim was to help the readers to evaluate and interpret the published Mössbauer data. Therefore, basic zero-magnetic field Mössbauer experiments were focused, and the Mössbauer parameters of isomer shift ( $\delta$ ) and quadrupole splitting ( $\Delta E_Q$ ) were mainly discussed in the review.

### 2. Theory

Mössbauer spectroscopy utilizes recoilless nuclear energy transition known as Mössbauer effect (Mössbauer, 1958), and which can be interpreted in terms of oxidation state and electronic spin state of the Mössbauer active nuclei. Iron (Fe) may be the most popular element studied by Mössbauer spectroscopy, and has been adopted for the Mössbauer investigation of Fe-containing metalloproteins for a long time. However, only the  $^{57}\text{Fe}$  isotope can be used for Mössbauer measurement, and its natural abundance is as low as 2.1%. For the excitation of  $^{57}\text{Fe}$  nuclear ground energy state,  $\gamma$ -radiation from the radioactive  $^{57}\text{Co}$  nuclide deposited onto a thin rhodium foil ( $^{57}\text{Co}/\text{Rh}$ ) has usually been used as an energy source. As radioactive  $^{57}\text{Co}$  with a half-life of 271.8 days is generally used as a light source for  $^{57}\text{Fe}$ -Mössbauer spectrometers, a new light source is required in every 2-3 years.

When the source or the observer (sample) moves at a speed of a few mm/s,  $\gamma$ -rays with slightly different energies from the  $^{57}\text{Co}$  source may interact with the nuclear energy transition of the  $^{57}\text{Fe}$  isotope in the sample (Fig. 1). The absorption of the energy is measured by the intensity change of the  $\gamma$ -ray, which is detected by the fluorescence. In the case of  $^{57}\text{Fe}$ , the excited nuclear energy state interacts with the surrounding electric field gradient anisotropically, and two different energy transitions occur. Therefore, the  $^{57}\text{Fe}$ -Mössbauer spectrum of the sample with one Fe species always results in a doublet, which is characterized as an isomer shift ( $\delta$ ) and quadrupole splitting ( $\Delta E_Q$ ) (Fig. 2).

\* Author for correspondence: jaehongh@cau.ac.kr

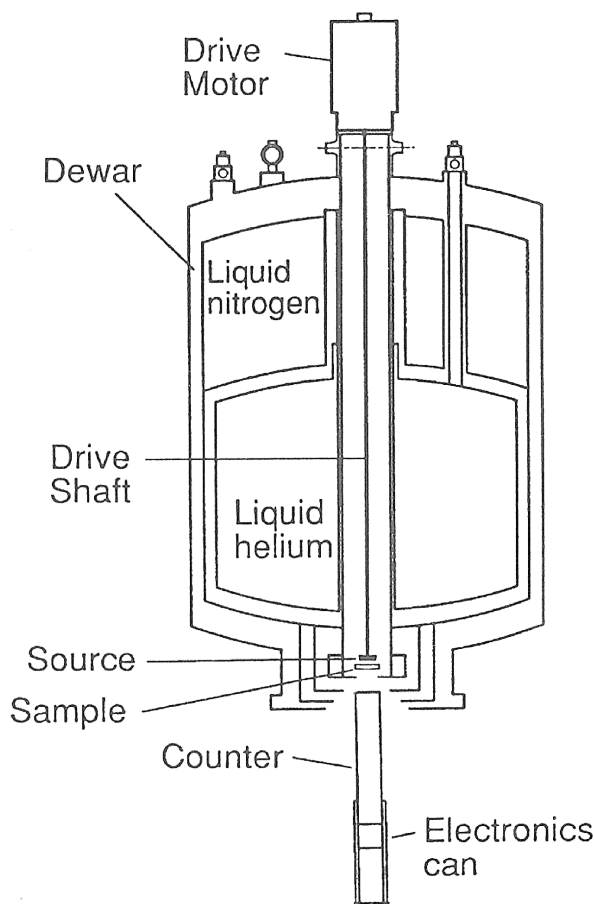


**Figure 1.** Cross section side view of major components of Mössbauer spectrometer (Moon *et al.*, 1996).

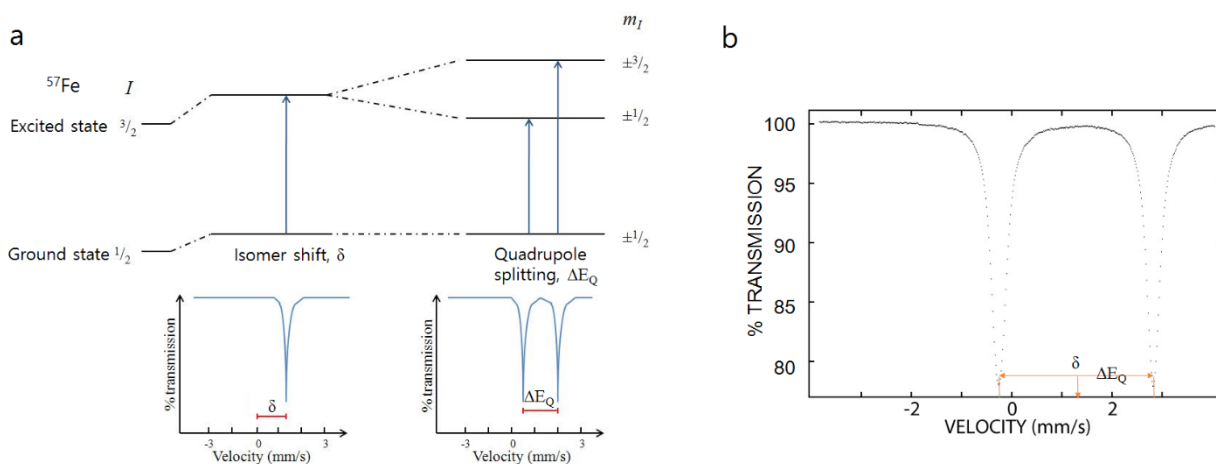


**Figure 2.** Mössbauer spectrum and Mössbauer parameters: a) energy transition by g-radiation and b) typical Mössbauer data extraction from the spectrum.

### 3. General aspects

Mössbauer spectroscopy has been used for chemical research since the late 1960's, following Rudolf Mössbauer's report in 1958. At that time, development of spectroscopic methodology preceded the standardization of data reporting methods. Experimental factors, including the  $^{57}\text{Co}$  source matrix, isomer shift reference, temperature, and sample preparation, were known to influence the Mössbauer data. Therefore, the data reported in the early

days, especially isomer shift  $\delta$ , should be recalibrated to the same reference. In this paper, Fe metal foil with  $^{57}\text{Co}/\text{Rh}$  source at room temperature was adopted as the isomer shift reference, *i.e.*  $d = 0$  mm/s, for data comparison (Table 1) (Shenoy and Wagner, 1978). Although temperature does influence the  $^{57}\text{Fe}$ -Mössbauer parameters of  $\delta$  and  $\Delta E_Q$ , the changes are usually insignificant and it appears no simple rules can explain them.

**Table 1.**  $\text{Fe}^{57}$ -Mössbauer isomer shift reference scales.

Reference Material	Absorber and source materials			
a-Fe, metallic Fe or Fe foil (300 K)	$\text{Na}_2\text{Fe}(\text{CN})_5\text{NO}\cdot 2\text{H}_2\text{O}$	Cr	Stainless steel	$\text{K}_4\text{Fe}(\text{CN})_6\cdot 3\text{H}_2\text{O}$
	-0.260(2)	-0.154(9)	-0.09(2)	-0.035(7)
	Rh	Pd	Cu	Pt
	+0.106(2)	+0.177(2)	+0.225(2)	+0.349(6)
$\text{Na}_2\text{Fe}(\text{CN})_5\text{NO}\cdot 2\text{H}_2\text{O}$ (300 K)	Cr	Stainless steel	$\text{K}_4\text{Fe}(\text{CN})_6\cdot 3\text{H}_2\text{O}$	a-Fe
	+0.106(9)	+0.17(2)	+0.225(7)	+0.260(2)
	Rh	Pd	Cu	Pt
	+0.366(2)	+0.437(2)	+0.485(2)	+0.609(6)

The Fe compound has been extensively studied by Mössbauer spectroscopy, and the relationship between oxidation state of the Fe center and  $\delta$  was generalized. For example, the reduced ferrous center,  $\text{Fe}(\text{II})$ , usually has electronic spin states of  $S = 2$  or  $S = 0$ , of which isomer shifts were found at the regions of  $d = 0.8 - 1.5$  mm/s and  $d = 0.25 - 0.55$  mm/s, respectively. The unusual  $S = 1$  state of  $\text{Fe}(\text{II})$  was reported to produce a Mössbauer signal at  $d = 0.3 - 0.4$  mm/s. The oxidation state of  $\text{Fe}(\text{I})$ , studied in organometallic complexes, was also found in biological systems, such as hydrogenase. The  $\text{Fe}(\text{I})$  ion may have an electronic spin state of  $S = 3/2$  or  $S = 1/2$ , and the isomer shifts of these species were found at the region of  $d = 1.95 - 2.05$  mm/s and  $d = 0.15 - 0.4$  mm/s, respectively. In the case of the low spin ferric center,  $\text{Fe}(\text{III})$ , usually observed from ferriheme, the isomer shifts are observed at around 0.27 mm/s, and are not much different from the high spin  $\text{Fe}(\text{III})$  complex.

#### 4. Biological Fe/S cluster

##### 4.1 Biological Fe/S proteins

Besides the structural functions, as observed from zinc finger proteins and calcium binding proteins, metal ions play many important roles in fundamental biological systems, such as photosynthesis, nitrogen fixation, and mitochondrial electron transport. One of the fundamental reactions that is essential for biological systems is electron transfer, and the Fe/S clusters and hemes are major cofactors for the function. There are various types of Fe/S clusters in biology, and most Fe/S clusters are classified based on the number of Fe atoms, as rubredoxin, ferredoxin-types, Rieske center, and aconitase-type  $[\text{3Fe4S}]$  clusters (Fig. 3). Other than electron transfer, the Fe/S proteins also catalyze many unique reactions, including nitrogen fixation, CO oxidation, methane oxidation, and hydrogen production (Holm *et al.*, 1996).

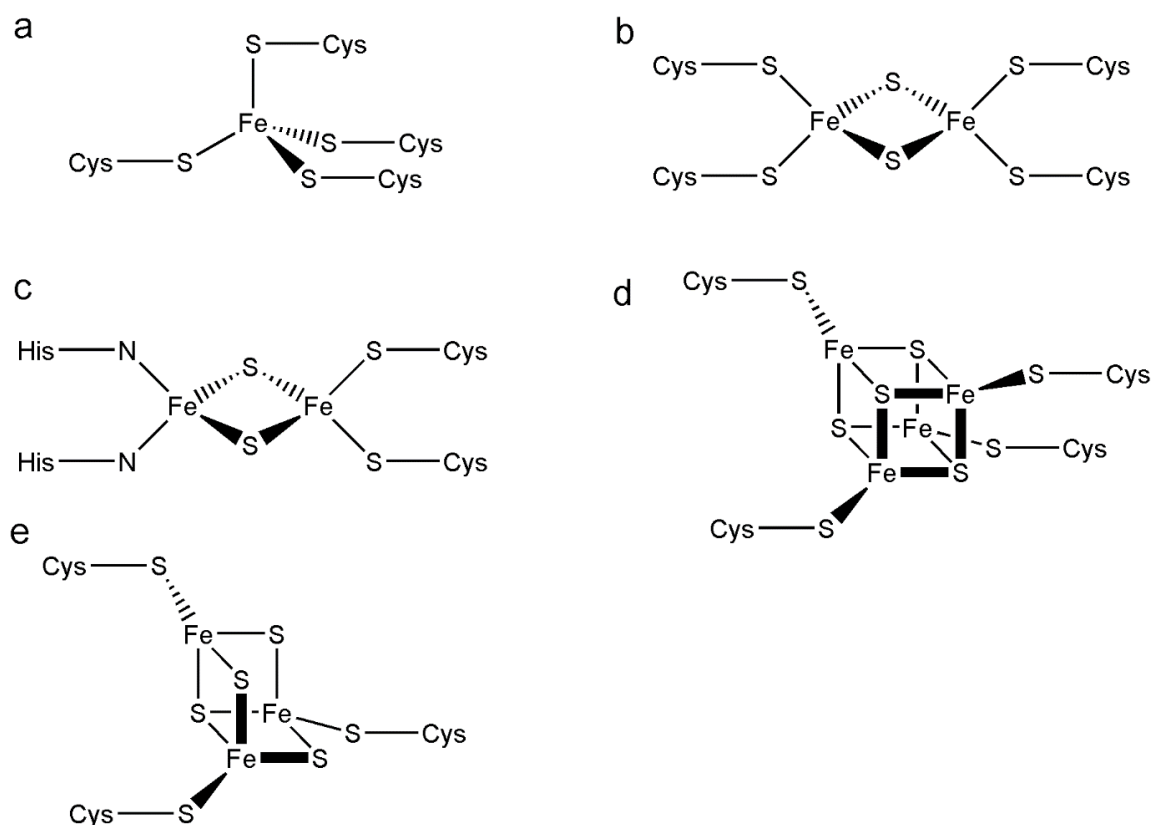


**Figure 3.** Structures of biological Fe/S clusters: a) Rubredoxin, b)  $[\text{2Fe2S}]$ -ferredoxin, c) Rieske-center, d)  $[\text{4Fe4S}]$ -ferredoxin, and e)  $[\text{3Fe4S}]$  cluster.

#### 4.2 Mössbauer isomer shifts of Fe/S proteins

Most Fe atoms in biological Fe/S clusters were known to have high spin electronic states, and general isomer shift values for the biological Fe/S clusters were reported by Beinert *et al.* (1997). Oxidized rubredoxin (Fig. 3a) with a high spin ferric center showed an isomer shift of  $d = 0.25$  mm/s and the reduced form, high spin ferrous ion, showed an isomer shift of  $d = 0.70$  mm/s. The [2Fe2S]ferredoxin (Fig. 3b) may form the oxidized or the reduced clusters. The oxidized  $[\text{Fe}_2\text{S}_2]^{+2}$  cluster has two ferric centers and the  $^{57}\text{Fe}$ -Mössbauer isomer shift was found at  $d = 0.27$  mm/s. Whereas, the reduced  $[\text{Fe}_2\text{S}_2]^+$  cluster has a ferrous and a ferric center, and the isomer shifts of  $d = 0.60$  mm/s and  $d = 0.35$  mm/s, respectively, were observed. For the oxidized  $[\text{Fe}_2\text{S}_2]^{2+}$  Rieske center (Fig. 3c), two Fe(III) centers were found at  $d = 0.27$  mm/s. The one electron reduced  $[\text{Fe}_2\text{S}_2]^+$  Rieske center with an Fe(II) and an Fe(III) ion showed signals at  $d = 0.72$  mm/s and  $d = 0.30$  mm/s, respectively. A similar relationship of the oxidation states of the Fe atom and the isomer shift was reported from the aconitase-type [3Fe4S] clusters (Fig. 3e). The oxidized  $[\text{Fe}_3\text{S}_4]^+$  cluster with three Fe(III) ions showed a signal at  $d = 0.27$  mm/s at 90 K, and the reduced  $[\text{Fe}_3\text{S}_4]^0$  cluster with

two Fe(III) and one Fe(II) centers showed two signals at  $d = 0.32$  mm/s (for Fe(III)) and  $d = 0.46$  mm/s (for the *valence-delocalized* Fe(II) + Fe(III) pair) at 15 K (Krabs, *et al.*, 2000). The relationship between the isomer shift and the oxidation state of the Fe atom valid for the cuboidal [4Fe4S] clusters (Fig. 3d) as well. Two *valence-delocalized* Fe(II) + Fe(III) pairs in the oxidized  $[\text{Fe}_4\text{S}_4]^{+2}$  cluster showed a signal at  $d = 0.45$  mm/s at 4.2 K. The reduced Fe(II) + Fe(II) pair and the other *valence-delocalized* Fe(II) + Fe(III) pair in the reduced  $[\text{Fe}_4\text{S}_4]^+$  cluster show  $d = 0.62$  mm/s and  $d = 0.49$  mm/s, respectively, at 110 K. It is noteworthy that the *valence-delocalized* Fe(II) + Fe(III) pair of the aconitase-type [3Fe4S] and the cuboidal [4Fe4S] clusters were found at  $d = 0.46$  mm/s and  $d = 0.45$  mm/s, respectively. The super-reduced  $[\text{Fe}_4\text{S}_4]^0$  cluster of the Fe protein from *Azotobacter vinelandii* was reported and its isomer shifts were found at  $d = 0.68$  mm/s (4.2 K),  $d = 0.65$  mm/s (130 K), and  $d = 0.62$  mm/s (200 K) (Yoo, *et al.*, 1999). Regardless of the experimental temperature, there is a strong correlation between the isomer shift and the oxidation state of the tetrahedral Fe center in the Fe/S clusters (Fig. 4).

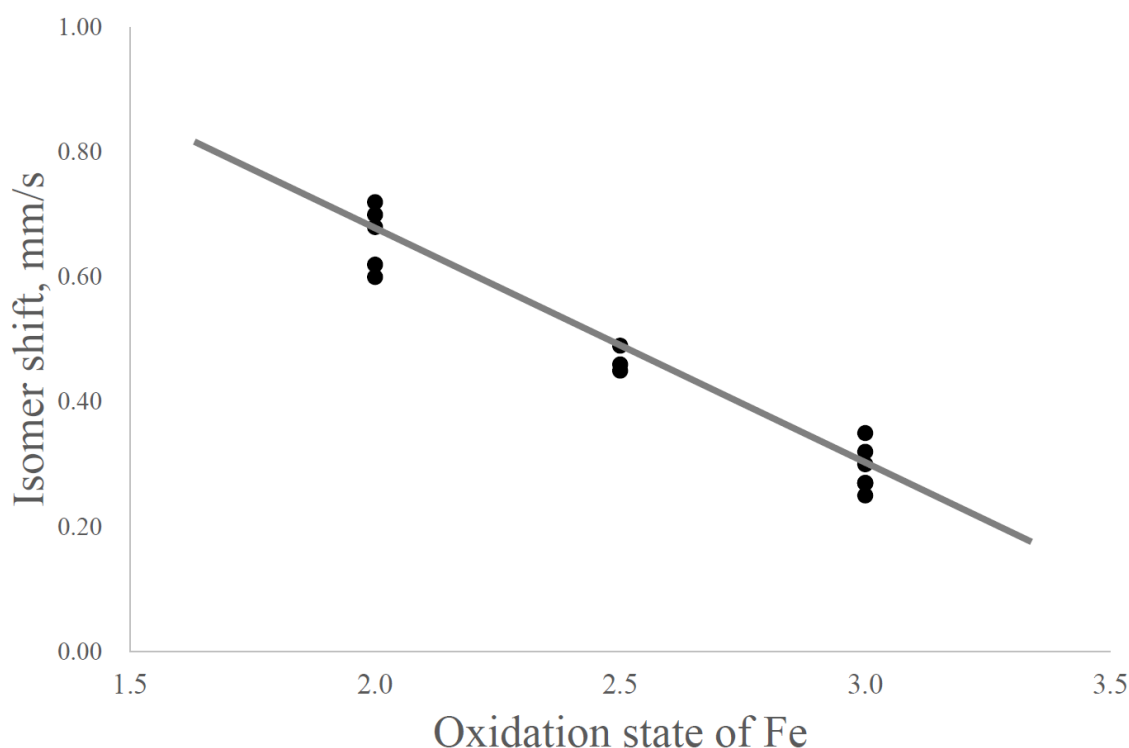


**Figure 4.** Relationship between oxidation state and  $^{57}\text{Fe}$ -Mössbauer isomer shift found from biological Fe/S clusters. Valence-delocalized Fe(II)-Fe(III) pairs were represented as +2.5 oxidation state.

## 5. Synthetic Fe/S clusters

### 5.1 Synthetic Fe/S clusters with SR, OR, or X ligands

Since the first chemical synthesis of the Fe/S cluster by Schunn *et al.* (1966), many synthetic Fe/S clusters have been synthesized to study the physical properties and the biological function of Fe/S clusters (Lee, *et al.*, 2014). The study of  $^{57}\text{Fe}$ -Mössbauer parameters of Fe/S clusters with

alkylthiolate ( $\text{SR}^-$ ) or halogenide ( $\text{X}^-$ ) has been carried out. The isomer shift of  $(\text{Ph}_4\text{P})_2[\text{Fe}_4\text{S}_4(\text{SPh})_4]$  (Fig. 5a) is shown at  $d = 0.43$  mm/s and its chloride analog (Fig. 5b) shows at  $d = 0.49$  mm/s at 77 K. The compound with different counter cation and ligand,  $(\text{Et}_4\text{N})_2[\text{Fe}_4\text{S}_4(\text{OPh})_4]$  (Fig. 5c), showed  $d = 0.50$  mm/s at 4.2 K.

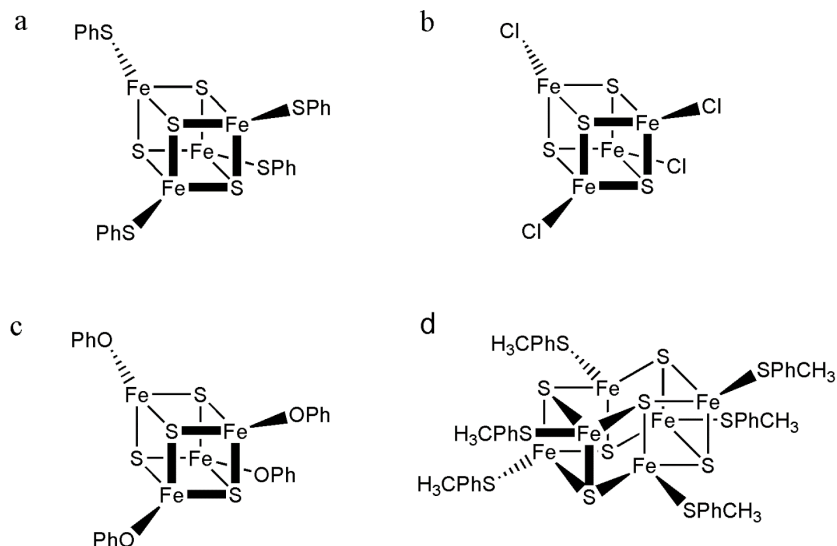


**Figure 5.** Structures of synthetic Fe/S clusters.

The Mössbauer study of the  $[\text{Fe}_6\text{S}_6]^{3+}$  cluster (Fig 5d) at 125 K was reported by Kanatzidis *et al.* (1985). For  $(\text{Et}_4\text{N})_3[\text{Fe}_6\text{S}_6(\text{S}-p\text{-MeC}_6\text{H}_4)_6]$  the isomer shift showed a peak at  $d = 0.440$  mm/s and its X analogs exhibited a positive isomer shift of  $d = 0.045 - 0.055$  mm/s. The chloride and the O- $p\text{-MeC}_6\text{H}_4$  analogs showed 0.055 mm/s and 0.036 mm/s of positive isomer shifts, respectively.

The synthetic clusters for the  $[\text{Fe}_3\text{S}_4]$  system (Fig 3e) have also been measured by Mössbauer spectroscopy to compare their parameters with biological clusters (Raebiger *et al.*, 1997). The  $[\text{Fe}_3\text{S}_4]^0$  clusters, regardless of their SR ligand species, show two quadrupole splittings of  $d = 0.48 - 0.49$  mm/s, for the Fe(II) + Fe(III) valence-delocalized pair, and  $d = 0.34 - 0.37$  mm/s, for the valence-localized Fe(III) center. These show a little higher isomer shift compared to the biological center by  $d = 0.02 - 0.03$  mm/s. When  $\text{Na}^+$  sits on the trigonal plane of three

S atoms, the isomer shift changes to  $d = 0.44$  mm/s for the Fe(II) + Fe(III) pair, and  $d = 0.41$  mm/s for the other Fe(III) when compared to the enzymatic system. The large  $\delta$  value observed from the Fe(III) center in the oxidized cluster was  $d = 0.32$  mm/s for *Desulfovibrio gigas*. Ferredoxin II and  $d = 0.34 - 0.41$  mm/s for the synthetic  $[\text{Fe}_3\text{S}_4]^0$  cluster show partial valence-delocalization of the ferric centers.

MacDonnell *et al.* (1995) studied the variations in Mössbauer parameters for two-, three-, and four-coordinate Fe(II) thiolate complexes. Regardless of the coordination number, it was found that the isomer shifts exclusively depended on the oxidation state of the Fe centers and the quadrupole splittings depended on the electronic spin state of Fe centers. As electronic spin of the Fe center increases, usually large quadrupole splitting ( $\text{DE}_Q$ ) values are observed.

## 5.2 Synthetic Fe/S clusters with phosphine ligands

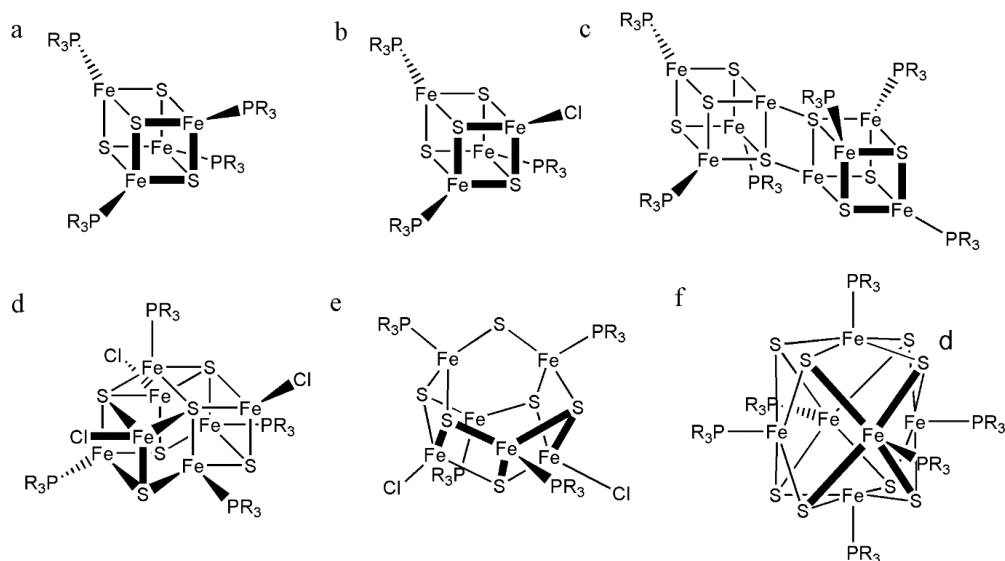


**Figure 6.** Structures of Fe/S clusters with phosphine ligands.

The reductive ligand substitution reactions of the synthetic  $[\text{Fe}_4\text{S}_4]$  clusters were determined, and the Mössbauer data of the reduced clusters were reported by Goh, *et al.* (1996). One thing to note is that  $[\text{Fe}_4\text{S}_4(\text{PR}_3)_4]$  BPh<sub>4</sub> clusters (Fig. 6a) showed similar isomer shift values to those of  $[\text{Fe}_4\text{S}_4]^{2+}$  clusters, even though its mean oxidation state was +2.25. It was proposed that the p-backbonding property of the Fe atom to the P atom increased the effective nuclear charge of the Fe center, which resulted in a decrease of the isomer shift. The changes in isomer shifts depended on the phosphine ligands species (from  $d = 0.41$  mm/s to  $d = 0.56$  mm/s), which confirmed again that the predominant factor of isomer shift change was Fe-P p-backbonding. The compound with  $\text{P}^t\text{Bu}_3$  shows the highest isomer shift of  $d = 0.56$  mm/s, and the others with  $\text{PcHex}_3$ ,  $\text{P}^i\text{Pr}_3$ , and  $\text{PcPent}_3$  show  $d = 0.48$  mm/s,  $d = 0.44$  mm/s, and  $d = 0.41$  mm/s, respectively. Based on these parameters, the isomer shifts of  $d = 0.601$  mm/s and  $d = 0.641$  mm/s (1:1) observed from  $[\text{Fe}_4\text{S}_4(\text{P}^t\text{Bu}_3)_3\text{Cl}]$  (Fig 6b) can be assigned as  $\text{Fe(III)Cl} + \text{Fe(II)}$  and  $\text{Fe(II)} + \text{Fe(II)}$  pairs respectively. The isomer shift of  $d = 0.601$  mm/s for the  $\text{Fe(III)Cl} + \text{Fe(II)}$  pair was much higher than the other  $\text{Fe(III)} + \text{Fe(II)}$  pairs with X, SR, or OR from  $[\text{Fe}_4\text{S}_4]$  or  $[\text{Fe}_3\text{S}_4]$  clusters by  $d = 0.10 - 0.17$  mm/s. The other  $\text{Fe(II)} + \text{Fe(II)}$  pair for  $d = 0.641$  mm/s appeared reasonable considering  $[\text{Fe}_4\text{S}_4(\text{PtBu}_3)_4]\text{BPh}_4$  showed  $d = 0.56$  mm/s. The edge-shared Fe/S double cubane,  $[\text{Fe}_8\text{S}_8(\text{PcHex}_3)_6]$  (Fig 6d), showed a very low average isomer shift at  $d = 0.55$  mm/s:  $d = 0.49$  mm/s for two  $\text{Fe(II)}$ ,  $d = 0.60$  mm/s for four  $\text{Fe(II)}$ , and  $d = 0.62$  mm/s for two  $\text{Fe(II)}$  even if all Fe atoms are  $\text{Fe(II)}$  formally. The smallest isomer shift of  $d = 0.49$  mm/s may be assigned to two Fe atoms in the  $[\text{2Fe2S}]$  intercubane unit. The Fe-Fe bond is much shorter than the other intracubane Fe-Fe bonds, such that the small isomer shift of  $d = 0.49$  mm/s may also be due to Fe-Fe

bonding.

There are high nuclearity synthetic Fe/S clusters with the  $[\text{Fe}_6\text{S}_6]$ ,  $[\text{Fe}_6\text{S}_8]$ , and  $[\text{Fe}_7\text{S}_6]$  cores. Most of them have a simple phosphine ligand, *i.e.*  $\text{PEt}_3$  and chloride ligands. The Mössbauer spectrum of  $[\text{Fe}_7\text{S}_6(\text{PEt}_3)_4\text{Cl}_3]$  (Fig. 6d), which has six  $\text{Fe(II)}$  and one  $\text{Fe(III)}$  centers, was fitted into three quadruplet splits. They were assigned as signals at  $d = 0.67$  mm/s for 3Fe-Cl,  $d = 0.36$  mm/s for 3Fe-P, and  $d = 0.36$  mm/s for the other Fe-P. The isomer shift of  $[\text{Fe}_6\text{S}_6(\text{PEt}_3)_4\text{Cl}_2]$  (Fig 6e), which has four  $\text{Fe(II)}$  and two  $\text{Fe(III)}$ , is assigned as  $d = 0.63$  mm/s for 2Fe-Cl,  $d = 0.34$  mm/s for 2Fe-P, and  $d = 0.32$  mm/s for 2Fe<sub>br</sub>-P. Its bromide and iodide analogs showed similar patterns of isomer shift distributions. For the comparison between ligands, all phosphine-ligated clusters were also measured. The cluster with five  $\text{Fe(II)}$  and one  $\text{Fe(III)}$ ,  $[\text{Fe}_6\text{S}_6(\text{PEt}_3)_6](\text{BF}_4)$ , was fitted with three centers of  $d = 0.41$  mm/s for 2Fe-P,  $d = 0.41$  mm/s for 2Fe-P, and  $d = 0.38$  mm/s for 2Fe<sub>br</sub>-P. The  $[\text{Fe}_8\text{S}_8(\text{PEt}_3)_6]^{n+}$ ,  $n = 0, +1, +2, +3$ , cluster has been studied by Mössbauer (Goddard *et al.*, 1996). The cluster shows that one electron reduction moves the isomer shift by  $d = \text{ca. } 0.04 - 0.05$  mm/s.

The Mössbauer study of the synthetic Fe/S clusters with phosphine ligands showed that the isomer shift was influenced by the nuclear effective charge that can be modified by phosphine ligands and the Fe backbonding property. For example, the tetrahedral  $(\text{Et}_4\text{N})[\text{FeCl}_3(\text{PEt}_3)]$  complex shows a doublet with Mössbauer parameters of  $\delta = 0.84$  mm/s and  $\Delta E_Q = 1.68$  mm/s (Fig. 7). The isomer shift value of the  $(\text{Et}_4\text{N})[\text{FeCl}_3(\text{PEt}_3)]$  was smaller than that of the  $(\text{Et}_4\text{N})_2[\text{FeCl}_4]$  ( $\delta = 0.90$  mm/s), and the quadrupole splitting value of 1.68 mm/s was much larger than that of the  $(\text{Et}_4\text{N})_2[\text{FeCl}_4]$  ( $\delta = 0.76$  mm/s) (Han and Nam, 2004).  $\text{Fe(II)}(\text{PEt}_3)_2\text{Cl}_2$  showed a signal of  $d = 0.65$  mm/s and  $\Delta E_Q = 2.90$  mm/s.

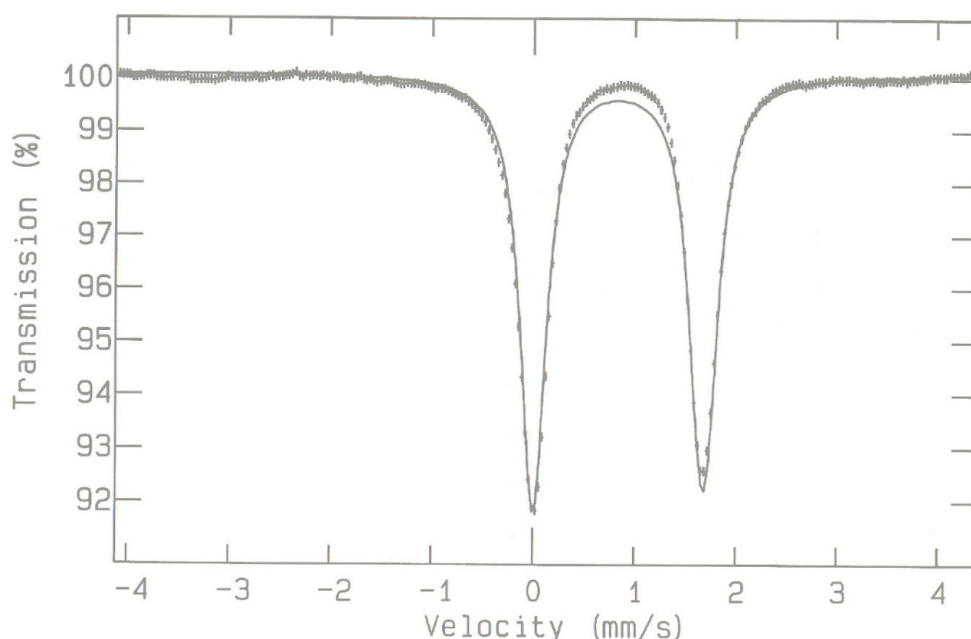


**Figure 7.**  $^{57}\text{Fe}$  Mössbauer spectrum of  $(\text{Et}_4\text{N})[\text{FeCl}_3(\text{PEt}_3)]$  at 125K in zero applied magnetic field. Cross marks are for observed data and solid line shows simulated graph fitted with one Fe center with Mössbauer parameters of  $\delta = 0.84$  mm/s and  $\Delta E_Q = 1.68$  mm/s.



### 5.3 Mo/Fe/S clusters

There are many biological Fe/S proteins containing heterometallic ions in the Fe/S cluster. For example, nitrogenase contains one Mo or V ion in the metal cofactor and Ni-hydrogenase contains an Ni ion in the catalytic center. Likewise, synthetic efforts for the new M/Fe/S clusters have produced many synthetic clusters. The simple

$[(\text{PPh}_3)_2\text{N}](\text{Et}_4\text{N})[(\text{MoS}_4)_2\text{Fe}]$  (Fig. 8a) showed an isomer shift of 0.38 mm/s and quadrupole splitting of 1.04 mm/s. The Mo(VI) and Fe(III) showed metal-metal interactions, as evident from the Mo-Fe distance, 2.740(1) Å (Coucounanis *et al.*, 1980). Therefore, the Fe(III) center appears to have an intermediate spin state.

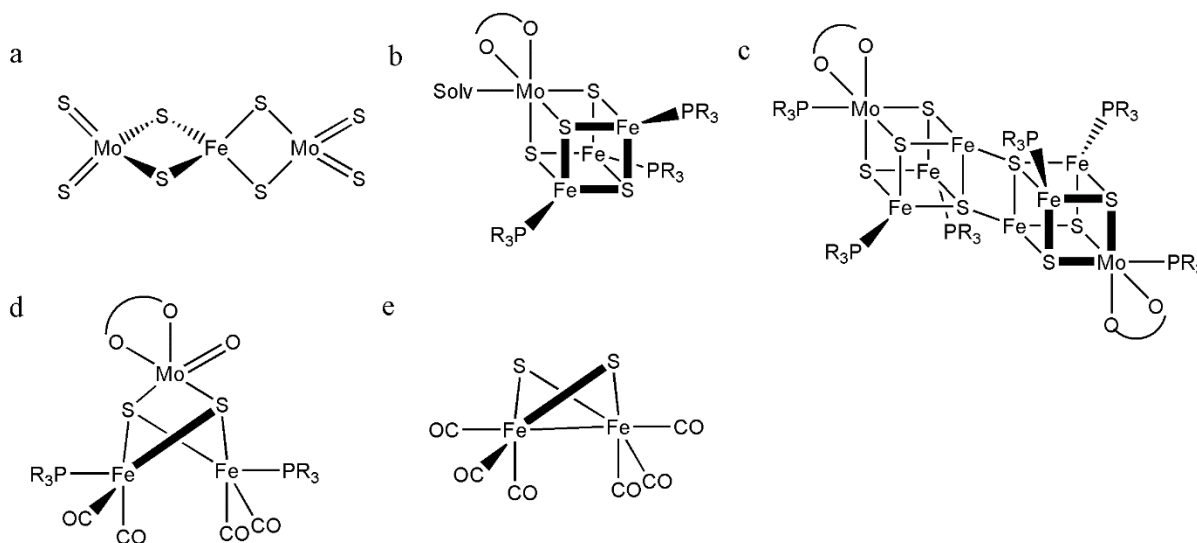


**Figure 8.** Structure of synthetic Mo/Fe/S clusters.

The  $[\text{MoFe}_3\text{S}_4]^{3+}$  cluster (Fig 8b), whose mean oxidation state of Fe is +2.67, shows  $d = 0.29$  mm/s with SR ligands. Chloride substitution gives a  $d = ca. 0.10$  mm/s isomeric shift and the same oxidation state cluster shows a doublet at  $d = 0.39$  mm/s. The one electron reduced cluster with SR ligand shows  $d = 0.41$  mm/s. The reduction of the cluster shifts  $d = 0.12$  mm/s isomeric shift per cluster and  $d = 0.04$  mm/s per Fe center (Osterloh *et al.*, 2000). Considering these, the phosphine substituted  $[\text{MoFe}_3\text{S}_4]^{2+}$  cluster can be compared and rationalized. The compound with a  $\text{P}^i\text{Bu}_3$  ligand on three Fe sites shows  $d = 0.53$  mm/s and  $d = 0.51$  mm/s isomer shifts in a 2:1 ratio as separate peaks. The *valence-localization* among Fe centers is consistent for the other analogs. The  $\text{P}^i\text{Pr}_3$  analog shows  $d = 0.49$  mm/s and  $d = 0.41$  mm/s (2:1), and  $\text{P}^i\text{Hex}_3$  at  $d = 0.48$  mm/s and  $d = 0.42$  mm/s (2:1). The average isomer shifts for the clusters are  $d = 0.52$  mm/s,  $d = 0.46$  mm/s, and  $d = 0.46$  mm/s, respectively. The larger value for the  $\text{P}^i\text{Bu}_3$  analog is not unexpected, as this is also found from the  $[\text{Fe}_4\text{S}_4]$  clusters. The same oxidation state cluster with SR ligand showed  $d = 0.41$  mm/s, and the phosphine ligand seems to move the isomer shift positively by  $d = 0.05 - 0.11$  mm/s.

The edge-shared  $[\text{MoFe}_3\text{S}_4]$  double cubane clusters,  $[(\text{Cl}_4\text{-cat})_2\text{Mo}_2\text{Fe}_6\text{S}_8(\text{PR}_3)]$  (Fig. 8c)  $\text{R} = \text{Et}, ^i\text{Pr}, ^i\text{Bu}$  can be analyzed as a  $[\text{MoFe}_3\text{S}_4]^{2+}$  clusters with two

phosphine and one S ligand. Two separate measurements for the  $\text{PET}_3$  analog show isomer shifts of  $d = 0.48$  mm/s and  $d = 0.45$  mm/s. From these data, the isomer shift by phosphine ligand cannot be observed. The  $[\text{MoFe}_3\text{S}_4]^{2+}$  cluster with the phosphine Fe ligand shows a similar isomer shift too. The  $^{99}\text{Ru}$  analog shows two doublets with  $d = 0.44$  mm/s and  $d = 0.38$  mm/s as well as  $\text{DE}_Q$  1.09 mm/s and  $\text{DE}_Q$  0.75 mm/s, respectively, in a 2:1 ratio. The isomer shift of the  $\text{P}^i\text{Pr}_3$  analog is found at  $d = 0.43$  mm/s and shows a smaller isomer shift value by  $d = 0.03 - 0.09$  mm/s. However, the difference could be due to one less phosphine ligand on the  $[\text{MoFe}_3\text{S}_4]$  cluster unit or the poor p-back bonding ability of Fe to  $\text{P}^i\text{Pr}_3$ .

### 5.4 Fe carbonyl clusters with low oxidation states

As shown by Morris and Schlaf (1994), the Mössbauer isomer shift  $\delta$  is influenced by a  $\pi$ -bonding contribution, which is controlled by ligand properties. The other ligand showing a strong  $\pi$ -bonding contribution is CO. The Mössbauer measurement of the  $(\text{Cl}_4\text{-cat})\text{Mo}(\text{O})\text{Fe}_2\text{S}_2(\text{CO})_4(\text{PET}_3)_2$  (Fig. 8d) showed two distinct Fe sites that have isomer shifts of 0.11 and 0.16 mm/s. The compounds have the same structural unit and were found from various organometallic compounds. The compounds in Table 2 (Bishop *et al.*, 1988) were synthesized from  $[\text{Fe}_2\text{S}_2(\text{CO})_6]^{2-}$  (Fig. 8e) and have at least one  $[\text{MoFe}_2\text{S}_2]$  subunit.

**Table 2.** Mössbauer parameters of various  $\text{MFe}_2\text{S}_2$  clusters with  $\text{Co}^{57}/\text{Rh}$  source at 78 K.

Compound	Oxidation state of Fe	d (mm/s)	$\text{DE}_Q$ (mm/s)
$(\text{NNMe}_2)_2(\text{PPh}_3)\text{MoFe}_2\text{S}_2(\text{CO})_6$	+1	0.033	0.800
$(\text{NNMePh})_2(\text{PPh}_3)\text{MoFe}_2\text{S}_2(\text{CO})_6$	+1	0.064	0.752
$(\text{NNMe}_2)_2(\text{PPh}_3)\text{WFe}_2\text{S}_2(\text{CO})_6$	+1	0.033	0.771
$(\text{NNMePh})_2(\text{PPh}_3)\text{WFe}_2\text{S}_2(\text{CO})_6$	+1	0.090	0.786
$(\text{NNMe}_2)_2(\text{PMe}_3)\text{MoFe}_2\text{S}_2(\text{CO})_6$	+1	0.060	0.707
$(\text{Ph}_2\text{CH}_2\text{CH}_2\text{PPh}_2)\text{NiFe}_2\text{S}_2(\text{CO})_6$	+1	0.051	0.723

**5.5 Fe/S clusters with low and intermediate spin states**

There are quite a few examples of low spin and intermediate spin ferrous and ferric compounds. Low spin ferrous compounds usually have a strong  $\pi$ -acceptor ligand, and the spin states of the ferric compounds seem to be influenced by the ligand geometry. High spin Fe(III) complexes, such as  $[\text{Fe}(\text{SEt})_4]^-$ , show isomer shifts of 0.25

mm/s and quadrupole splitting of 0.62 mm/s at 4.2K. The intermediate spin ( $S = 3/2$ ) complex of  $(\text{Et}_4\text{N})_2[\text{Fe}_2(\text{BDT})_4]$  ( $\text{BDT} = \text{C}_6\text{H}_4\text{S}_2$ ) showed a smaller isomer shift than its high spin analog,  $(\text{Et}_4\text{N})_2[\text{Fe}_2(\text{MP})_4] \cdot 2\text{MeCN}$  ( $\text{MP} = \text{C}_6\text{H}_4\text{OS}$ ) by ca. 0.1 mm/s (Kang *et al.*, 1988). Goh *et al.* (1994) also reported Mössbauer parameters for the  $[\text{Fe}_4\text{S}_4]^{+2}$  cluster with low spin  $\text{Fe}^{\text{II}}$  centers (Table 3).

**Table 3.** Mössbauer parameters for  $[\text{Fe}_4\text{S}_4\text{L}_2(\text{t-BuCN})_6]$  with  $\text{Co}^{57}/\text{Rh}$  source at 77 K.

Ligand	Site, spin state	d (mm/s)	$\text{DE}_Q$ (mm/s)
$\text{Cl}^-$	$\text{Fe}^{\text{III}}$ , HS	0.41	0.60
	$\text{Fe}^{\text{II}}$ , LS	0.19	0.45
$\text{Br}^-$	$\text{Fe}^{\text{III}}$ , HS	0.40	0.64
	$\text{Fe}^{\text{II}}$ , LS	0.18	0.46
$p\text{-MeC}_6\text{H}_4\text{O}^-$	$\text{Fe}^{\text{III}}$ , HS	0.37	0.64
	$\text{Fe}^{\text{II}}$ , LS	0.17	0.48
$\text{PhS}^-$	$\text{Fe}^{\text{III}}$ , HS	0.34	0.39
	$\text{Fe}^{\text{II}}$ , LS	0.16	0.43
$p\text{-MeC}_6\text{H}_4\text{S}^-$	$\text{Fe}^{\text{III}}$ , HS	0.33	0.44
	$\text{Fe}^{\text{II}}$ , LS	0.18	0.48
$t\text{-BuS}^-$	$\text{Fe}^{\text{III}}$ , HS	0.35	0.54
	$\text{Fe}^{\text{II}}$ , LS	0.17	0.49
$\text{EtS}^-$	$\text{Fe}^{\text{III}}$ , HS	0.29	0.67
	$\text{Fe}^{\text{II}}$ , LS	0.19	0.46

**6. Conclusions**

$^{57}\text{Fe}$ -Mössbauer spectroscopy can provide physical properties of Fe-containing proteins, and the relationship between the oxidation state and isomer shift  $\delta$  was well established, especially for the Fe/S clusters. Most Fe atoms in biological Fe/S clusters have a high spin state, and the oxidation states of single Fe ions and valence-delocalized Fe centers show linear responses to the isomer shift (Fig 4). The isomer shift is mainly governed by the effective nuclear charge changes resulting from the oxidation state change and ligand substitutions. Therefore, coordination environment changes and substrate binding to the Fe centers can be monitored by the isomer shift changes. Another factor influencing the electron density around the Fe center is metal-metal bonding between two metal ions. In this regard,  $^{57}\text{Fe}$ -Mössbauer spectroscopy of the Fe/S and Mo/Fe/S clusters can also provide evidence of the metal-metal bonding interactions.

**Acknowledgement**

This research was supported by the National Research Foundation of Korea (NRF) funded by the Korean Government (NRF-2010-0020984).

**References**

- Beinert, H. Holm, R. H. and Munck, E. 1997. Iron-sulfur clusters: nature's modular, multipurpose structures. *Science* 277, 653-659.
- Bishop, P. T. Dilworth, J. R. and Morton, S. 1988. Iron-molybdenum and iron-tungsten sulphido clusters containing hydrazido(2-) ligands. The synthesis and X-ray crystal and molecular structure of  $[\{\text{Fe}(\text{CO})_3(\mu_3\text{-S})\}_2\text{Mo}(\text{NNMe}_2)_2(\text{PPh}_3)](\text{Fe-Fe}) \cdot \text{CH}_2\text{Cl}_2$ . *Journal of Organometallic Chemistry* 341, 373-380.
- Coucovanis, D. Simhon, E. D. and Baenziger, N. C. 1980. Successful isolation of a reduced tetrathiomallate complex. Synthesis and structural characterization of the  $[(\text{MoS}_4)_2\text{Fe}]^{3-}$  trianion. *Journal of the American Chemical Society* 102, 6644-6646.
- Filatov, M. 2009. First principles calculation of Mössbauer isomer shift. *Coordination Chemistry Reviews* 253, 594-605.
- Goddard, C. A. Long, J. R. and Holm, R. H. 1996. Synthesis and characterization of four consecutive members of the five-member  $[\text{Fe}_6\text{S}_8(\text{PEt}_3)_6]^{n+}$  ( $n = 0-4$ ) cluster electron transfer series. *Inorganic Chemistry* 35, 4347-4354.



- Goh, C. Segal, B. M. Huang, J. Long, J. R. and Holm, R. H. 1996. Polycubane clusters: Synthesis of  $[\text{Fe}_4\text{S}_4(\text{PR}_3)_4]^{1+.0}$  ( $\text{R} = \text{Bu}^t, \text{Cy}, \text{Pr}^i$ ) and  $[\text{Fe}_4\text{S}_4]^0$  core aggregation upon loss of phosphine. *Journal of the American Chemical Society* 118, 11844-11853.
- Goh, C. Weigel, J. A. and Holm, R. H. 1994. The [2:2] site-differentiated clusters  $[\text{Fe}_4\text{S}_4\text{L}_2(\text{RNC})_6]$  containing two low-spin iron(II) sites. *Inorganic Chemistry* 33, 4861-4868.
- Gütlich, P. Bill, E. and Trautwein, A. X. 1978. Mössbauer spectroscopy and transition metal chemistry. Fundamentals and application. Springer-Verlag, Berlin, pp.569.
- Han, J. and Nam, W. 2004. Synthesis and structure of the new Fe complex,  $[\text{Fe}^{\text{II}}\text{Cl}_3(\text{PEt}_3)]^-$ . *Bulletin of the Korean Chemical Society* 25, 910-912.
- Holm, R. H. Kennepohl, P. and Solomon, E. I. 1996. Structural and functional aspects of metal sites in biology. *Chemical Reviews* 96, 2239-2314.
- Kanatidis, M. G. Hagen, W. R. Dunham, W. R. Lester, R. K. and Coucouvanis, D. 1985. Metastable iron/sulfur clusters. The synthesis, electronic structure, and transformations of the  $[\text{Fe}_6\text{S}_6(\text{L})_6]^{3-}$  clusters ( $\text{L} = \text{Cl}^-, \text{Br}^-, \text{I}^-, \text{RS}^-, \text{RO}^-$ ) and the structure of  $[(\text{C}_2\text{H}_5)_4\text{N}]_3[\text{Fe}_6\text{S}_6\text{Cl}_6]$ . *Journal of the American Chemical Society* 107, 953-961.
- Kang, B. S. Weng, L. H. Wang, F. Guo, Z. Huang, L. R. Huang, Z. Y. and Liu, H. Q. 1988. Pentacoordinate iron-sulfur complexes. Structure and spectroscopic and electrochemical properties of phenoxy- and thiophenoxy-bridged binuclear complexes. *Inorganic Chemistry* 27, 1128-1130.
- Krabs, C. Henshaw, T. F. Cheek, J. Huynh, B. H. and Broderick, J. B. 2000. Conversion of 3Fe-4S to 4Fe-4S clusters in native pyruvate formate-lyase activating enzyme: Mössbauer characterization and implications for mechanism. *Journal of the American Chemical Society* 122, 12497-12506.
- Lee, S. C. Lo, W. and Holm, R. H. 2014. Developments in the biomimetic chemistry of cubane-type and higher nuclearity iron-sulfur clusters. *Chemical Reviews* 114, 3579-3600.
- MacDonnell, F. M. Ruhlandt-Senge, K. Ellison, J. J. Holm, R. H. and Power, P. P. 1995. Sterically encumbered iron(II) thiolate complexes: Synthesis and structure of trigonal planar  $[\text{Fe}(\text{SR})_3]^-$  ( $\text{R} = 2,4,6\text{-t-Bu}_3\text{C}_6\text{H}_2$ ) and Mössbauer spectra of two- and three-coordinate complexes. *Inorganic Chemistry* 34, 1815-1822.
- Moon, N. Coffin, C. T. Steinke, D. C. Sands, R. H. and Dunham, W. R. 1996. A Mössbauer spectrometer for the study of natural abundance iron proteins. *Nuclear Instruments and Methods in Physics Research Section B: Beam Interactions with Materials and Atoms* 119, 555-564.
- Morris, R. H. and Schlaf, M. 1994.  $\pi$ -Bonding of the dihydrogen ligand -probed by Mössbauer spectroscopy. *Inorganic Chemistry* 33, 1725-1726.
- Mössbauer, R. L. 1958. Kernresonanzfluoreszenz von Gammastrahlung in Ir191. *Zeitschrift für Physik A* (in German) 151, 124-143.
- Osterloh, F. Segal, B. M. Achim, C. and Holm, R. H. 2000. Reduced mono-, di-, and tetracubane-type clusters containing the  $[\text{MoFe}_3\text{S}_4]^{2+}$  core stabilized by tertiary phosphine ligation. *Inorganic Chemistry* 39, 980-989.
- Raebiger, J. W. Crawford, C. A. Zhou, J. and Holm, R. H. 1997. Reactivity of cubane-Type  $[(\text{OC})_3\text{MFe}_3\text{S}_4(\text{SR})_3]^{3-}$  clusters ( $\text{M} = \text{Mo}, \text{W}$ ): Interconversion with cuboidal  $[\text{Fe}_3\text{S}_4]^0$  clusters and electron transfer. *Inorganic Chemistry* 36, 994-1003.
- Schunn, R. A., Fritchie, C. J., Jr. and Prewitt, C. T. 1966. Syntheses of some cyclopentadienyl transition metal sulfides and the crystal structure of  $(\text{C}_5\text{H}_5\text{FeS})_4$ . *Inorganic Chemistry* 5, 892-899.
- Shenoy, G. K. and Wagner, F. E. 1978. Mössbauer isomer shift. North-Holland Publishing Company. Amsterdam, pp.956.
- Vertes, A., Korecz, L. and Burger, K. 1979. Mössbauer Spectroscopy, Part V of Studies in Physical and Theoretical Chemistry. Elsevier Publishing Co., Amsterdam, pp.432.
- Yoo, S. J. Angove, H. C. Burgess, B. K. Hendrich, M. P. and Münck, E. 1999. Mössbauer and integer-spin EPR studies and spin-coupling analysis of the  $[\text{4Fe-4S}]^0$  cluster of the Fe protein from *Azotobacter vinelandii* nitrogenase. *Journal of the American Chemical Society* 121, 2534-2545.